Theoretical Analysis of Susceptibility of Ferritic Stainless Steel to Intergranular Corrosion Caused by Welding†

Hiroshi ARAI*, Seiichi TAKEDA* and Yoshiaki ARATA**

Abtract

The carbide precipitation and the susceptibility to intergranular corrosion in ferritic stainless steels were studied theoretically. The thermodynamic data by many references are formulated and the carbide precipitation at the grain boundary was calculated by using a local equilibrium model. Ferritic stainless steel (17Cr-0.01C) becomes susceptible 10^{-5} times more quickly than austenitic one (18Cr-9Ni-0.03C). The phase diagrams for Fe-Cr-C steels on the extremely low-C side were calculated for 1173K to 1473K. Using these diagrams, a strange phenomenon that lower the C content of ferritic stainless steel (i.e. 17Cr-0.07C to 0.03C), the more susceptible it becomes could be explained. It is also showed that the cause of corrosion depends on whether austenitic phase is created or not in the steel at the time of welding.

KEY WORDS: (Carbide Precipitation) (Intergranular Corrosion) (Equilibrium Model) (Ferritic Stainless Steel) (TTS Curve) (Phase Diagram)

1. Introduction

Ferritic stainless steel gives faster precipitation of carbide and has higher susceptibility to intergranular corrosion than does austenitic stainless steel. For this reason, the ferritic stainless steel was not generally used for the purposes for which welding is required. In recent years, very low C and N steel what is called "super ferritic stainless steel" was developed to make up for these disadvantages. Even such a steel cannot be prevented from intergranular corrosion unless stabilizing elements such as Ti and Nb are added. Moreover a strange phenomenon is observed in 17%Cr stainless steel that with the decreases in the C and N contents, the steel grows more vulnerable to intergranular corrosion[1]. Thus, the problem of carbide precipitation in ferritic stainless steel still remains important.

However, the studies on this problem are quite few, as compared with the studies on the similar problem in the austenitic counterpart. Probably this is because the very low solubility limit of C and high diffusion rate of C make experimental studies difficult, and because an increased C content generates an austenitic phase before C reaches the solubility limit, thus making it necessary to analyze the two-phase effect. Under these circumstances, an effective method is to prepare and analyze a thermodynamic model. The authors had scanned the references which dealt with the thermodynamic data such as the activities of Cr and C and the formation energy of carbide in stainless steel, then had made up these data to mathematical formulas so that these data can be easily utilized, and analysed, using a local equilibrium precipitation model[2].

This report deals with the theoretical calculations on the time-temperature sensitization diagrams for the intergranular corrosion of ferritic stainless steel, and at the same time it deals with the analysis why low-C/low-N steel becomes highly susceptible to the intergranular corrosion.

2. Thermodynamic Data

Thermodynamic data such as the activity coefficients of Cr, Fe and C in stainless steel, the carbide-forming energy and the diffusion rate of Cr are available from the previous report[2] presented by some of the present authors.

2.1 Activity coefficient of Cr

In the austenite:

$$\gamma_{Cr}^{\gamma} = \exp\left[2330/T - 1.111 + (X_{Cr} + 0.3)X_{Ni}\right] \quad (1)$$

In the ferrite:

$$\gamma_{Cr}^{\alpha} = \exp\left[(3250/T - 1.95 + 1.24X_{Cr})(1 - X_{Cr})^2\right] \quad (2)$$

where T is absolute temperature; X_{Cr} and X_{Ni} are mole fractions of Cr and Ni respectively.

2.2 Activity coefficient of Fe

In the austenite:

$$\gamma_{Fe}^{\gamma} \simeq 1.0 \quad (3)$$

In the ferrite:

† Received on May 6, 1987
* Nippon Metal Industry Co., Ltd.
** Professor

Transactions of JWRI is published by Welding Research Institute of Osaka University, Ibaraki, Osaka 567, Japan

$$\gamma^{\alpha}_{Fe} = \exp\left[(3250/T - 2.57 + 1.24X_{Cr})X_{Cr}{}^2\right] \quad (4)$$

2.3 Activity coefficient of C

In the austenite:

$$\gamma^{\gamma}_{C} = \exp\left[(5100/T - 1.845) + (4.89 - 17687/T)X_{Cr} + (-0.86 + 7660/T)X_{Ni}\right] \quad (5)$$

In the ferrite:

$$\gamma^{\alpha}_{C} = \exp\left[(13440/T - 6.277) + (-21600/T + 11.7)X_{Cr}\right] \quad (6)$$

2.4 Formation energy of carbide

The first carbide precipitating in stainless steel is (Cr, Fe)$_{23}$C$_6$. In order to estimate the formation energy for this complex carbide, it is convenient to think of $Cr_{23}C_6$ and assumptive $Fe_{23}C_6$ and to use an approximation of the regular solution for calculation. Namely:

$$\Delta G_f^{MC}{}_{6/23} = Y_{Cr}\Delta^{\circ}G_f^{CrC}{}_{6/23} + (1 - Y_{Cr})\Delta^{\circ}G_f^{FeC}{}_{6/23} + RT\left[Y_{Cr}\ln Y_{Cr} + (1 - Y_{Cr})\ln(1 - Y_{Cr})\right] \quad (7)$$

where Y_{Cr} is mole fraction of Cr in the metal composition of carbide. $\Delta^{\circ}G_f^{FeC}{}_{6/23}$ and $\Delta^{\circ}G_f^{CrC}{}_{6/23}$ are formation energy of $Cr_{23}C_6$ and $Fe_{23}C_6$, respectively, which can be given as follows.

$$\Delta^{\circ}G_f^{CrC}{}_{6/23} = -13993 - 3.33T \quad \text{J/mol} \quad (8)^{3)}$$

$$\Delta^{\circ}G_f^{FeC}{}_{6/23} = \Delta^{\circ}G_f^{CrC}{}_{6/23} + 4000 + 10T \quad \text{J/mol} \quad (9)$$

2.5 Diffusion coefficient of Cr

Lattice diffusion coefficient in the austenite:

$$D^{r}_{Cr} = 0.13\exp(-264000/RT) \ \text{cm}^2/\text{s} \quad (10)$$

Lattice diffusion coefficient in the ferrite:

$$D^{\alpha}_{Cr} = 0.46\exp(-219600/RT) \ \text{cm}^2/\text{s} \quad (11)$$

3. Intergranular Precipitation of Carbide

The carbide precipitation in stainless steel takes place first in grain boundaries where the increment of interface tension energy is less. Sometimes transgranular precipitation simultaneously takes place. However, since the intergranular precipitation is dominant in the initial stage of precipitation, it is possible to discuss with no regard to the transgranular precipitation.

Let us assume that the carbide precipitating in the grain boundary is (Cr, Fe)$_{23}$C$_6$, and let Y_{Cr} represent the mole fraction of Cr in the metal components of carbide. X^{i}_{Cr}, X^{i}_{Fe} and X^{i}_{Ni} represent the contents of Cr, Fe and Ni respectively, which equilibrate locally with carbide in the grain boundaries. Their initial contents in matrix are represented by X°_{Cr}, X°_{Fe}, X°_{Ni}, and X°_{C}. X_C represents the C content which changes with carbide precipitation. The values for these items can be related to one another by equations of the equilibrium conditions and a differential equations which describe Cr diffusion from the matrix to the grain boundary. Since, Ni is not contained in the precipitation, it is assumed that $X^{i}_{Ni} \simeq X^{\circ}_{Ni}$.

3.1 Relationship between grain boundary composition and carbide composition

As C diffuses quite faster than Cr, the activity coefficient of C in the grain boundary can be regarded as equal to that in the matrix. Therefore, the activity of Cr, Fe and C in the grain boundary can be expressed as follows:

In the case of austenitic steel:

$$a^{\gamma}_{Cr} = \exp\left[(2330/T - 1.111 + (X_{Cr} + 0.3)X_{Ni}\right]X^{i}_{Cr} \quad (12)$$

$$a^{\gamma}_{Fe} = X^{\circ}_{Fe} \quad (13)$$

$$a^{\gamma}_{C} = \exp\left[(5100/T - 1.845) + (4.89 - 17687/T)X^{\circ}_{Cr} + (-0.86 + 7660/T)X^{\circ}_{Ni}\right]X_C \quad (14)$$

In the case of ferritic steel:

$$a^{\alpha}_{Cr} = \exp\left[(3250/T - 1.95 + 1.24X^{i}_{Cr})(1 - X^{i}_{Cr})^2\right]X^{i}_{Cr} \quad (15)$$

$$a^{\alpha}_{Fe} = \exp\left[(3250/T - 2.57 + 1.24X^{i}_{Cr})X^{i}_{Cr}{}^2\right]X^{i}_{Fe} \quad (16)$$

$$a^{\alpha}_{C} = \exp\left[(13440/T - 6.277) + (-21600/T + 11.7)X^{\circ}_{Cr}\right]X_C \quad (17)$$

Therefore

$$RT(\ln a_{Cr} + 6/23 \cdot \ln a_C) = \Delta^{\circ}G_f^{CrC}{}_{6/23} + RT\ln Y_{Cr} \quad (18)$$

and

$$RT(\ln a_{Fe} + 6/23 \cdot \ln a_C) = \Delta^{\circ}G_f^{FeC}{}_{6/23} + RT\ln(1 - Y_{Cr}) \quad (19)$$

give the following equations:

For austenitic steel:

$$RT\left[2330/T - 1.111 + (X^{i}_{Cr} + 0.3)X^{\circ}_{Ni} + \ln\left\{X^{i}_{Cr}/(1 - X^{i}_{Cr} - X^{\circ}_{Ni})\right\} + \ln\left\{(1 - Y_{Cr})/Y_{Cr}\right\}\right] = -4000 - 10T \ \text{J/mol} \quad (20)$$

For ferritic steel:

$$RT[(3250/T-1.95+1.24X^{i}_{Cr})(1-X^{i}_{Cr})^2 + \ln\{X^{i}_{Cr}/(1-X^{i}_{Cr}-X^{\circ}_{Ni})\} + \ln\{(1-Y_{Cr})/Y_{Cr}\}] = -4000-10T \text{ J/mol} \quad (21)$$

3.2 Relationship between grain boundary compositions and the amount of carbide precipitated

The amount of carbide precipitated is determined by the Cr diffusion into the grain boundary. If the grains are approximated by a sphere (with a radius of r_0), and if the diffusion region of Cr near the grain boundary is assumed to be sufficiently small as compared to the grain sizes, then it is possible to handle the diffusion as lamellar (flat disk) precipitation. If S represents a half of average thickness of precipitated carbide, then S can be given by the following equation[4]:

$$S = \frac{2(X^{\circ}_{Cr}-X^{i}_{Cr})}{X^{P}_{Cr}-X^{i}_{Cr}} \cdot \sqrt{\frac{D_{Cr}\,t}{\pi}} \quad (22)$$

where X^{P}_{Cr} is the calculated volume concentration of Cr in carbide, same as in the case of Cr concentration (mole fraction) in the matrix. X^{P}_{Cr} is given by the following equation:

$$X^{P}_{Cr} = 23V_m/(23V_m+6V_C)\cdot Y_{Cr} \quad (23)$$

where V_m is molar volume of (Cr, Fe), and V_C is the molar volume of C, and $(23V_m + 6V_C)$ is the molar volume of $(Cr, Fe)_{23}C_6$.

When the thickness of the grain boundary carbide has been determined in this manner, the mole fraction of carbon fixed as carbide (ΔX_C) is obtained from the volume percent of carbide, the mole fraction of C in carbide and the density relationship between matrix and carbide, using the following equation:

$$\Delta X_C = 4\pi r_0^2 S/(\frac{4}{3}\pi r_0^3)\cdot(\frac{6}{23})\cdot(\frac{23V_m}{23V_m+6V_C}) = \frac{6}{r_0}\cdot\frac{X^{\circ}_{Cr}-X^{i}_{Cr}}{Y_{Cr}-X^{i}_{Cr}+X^{i}_{Cr}(6V_C/23V_m)}\cdot\sqrt{\frac{D_{Cr}\,t}{\pi}}\cdot\frac{6}{23} \simeq \frac{6}{23}\cdot\frac{6}{r_0}\cdot\frac{X^{\circ}_{Cr}-X^{i}_{Cr}}{Y_{Cr}-X^{i}_{Cr}}\cdot\sqrt{\frac{D_{Cr}t}{\pi}} \quad (24)$$

3.3 Relationship between activity of C and grain boundary composition

With the progress in carbide precipitation, the solute C in the matrix decreases, and the activity of C lowers. Putting the thermodynamic data and ΔX_C shown in equation (24) to the equation (18), the following equations are obtained:

For austenitic steel:

$$RT[2330/T-1.111+(X^{i}_{Cr}+0.3)X^{\circ}_{Ni} + 6/23\cdot\{5100/T-1.845+(4.89-17687/T)X^{\circ}_{Cr} + (-0.86+7660/T)X^{\circ}_{Ni}\}+\ln(X^{i}_{Cr}/Y_{Cr}) + 6/23\cdot\ln(X^{\circ}_{C}-\Delta X_C)] = -13993-3.33T \text{ J/mol} \quad (25)$$

For ferritic steel:

$$RT[(3250/T-1.95+1.24X^{i}_{Cr})(1-X^{i}_{Cr})^2 + 6/23\cdot\{13440/T-6.277 + (-21600/T+11.7)X^{\circ}_{Cr}\}+\ln(X^{i}_{Cr}/Y_{Cr}) + 6/23\cdot\ln(X^{\circ}_{C}-\Delta X_C)] = -13993-3.33T \text{ J/mol} \quad (26)$$

3.4 Examples of calculation

After the foregoing preparations are completed, the three unknown quantities, X^{i}_{Cr}, Y_{Cr} and ΔX_C, can be obtained as the function of elapsed time, t, by solving the simultaneous equations of either (20), (24) and (25) or (21), (24) and (26). **Figures 1** and **2** show the results of calculation on 17.7Cr-9.3Ni-0.03C steel as an example of austenitic stainless steel and 17Cr-0.01C steel as an example of ferritic stainless steel.

4. Appraisal of the Susceptibility to Intergranular Corrosion

For practical purpose, the largest problem at grain boundary precipitation of carbide is the increase in susceptibility to intergranular corrosion found in the heat affected zone of the weld. Since it is considered that this susceptibility is related to the degree of Cr deficiency at the grain boundary and the extent of Cr depleated zone, they are joined to define an index, I, which is given by the following equation:

$$I = (X^{t}_{Cr} - X^{i}_{Cr})\Delta X_C \quad (27)$$

where X^{t}_{Cr}, is the critical Cr level at which the stainless steel rapidly loses its anti-corrosive property. Let us assume now that this level is 0.15. At $I = 10^{-5}$ (mole fraction)^2, the time-temperature sensitization (TTS) curves were calculated for the austenitic stainless steel of 17.7Cr-9.4Ni-0.03C and for the ferritic stainless steels of 17Cr-0.005C, 17Cr-0.010C, 17Cr-0.015C, 17Cr-0.020C and 17Cr-0.03C. **Figures 3** and **4** show the results. The TTS curves of ferritic stainless steels shifts remarkably to

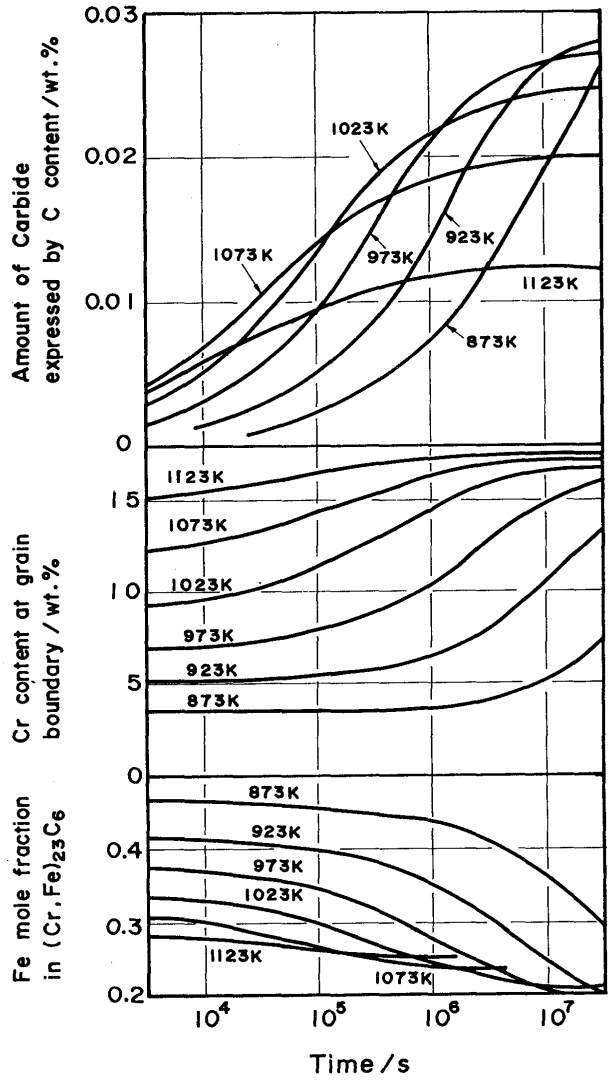

Fig. 1 Calculated results for SUS304L.
(17.7Cr-9.4Ni-0.03C, grain size: 6)

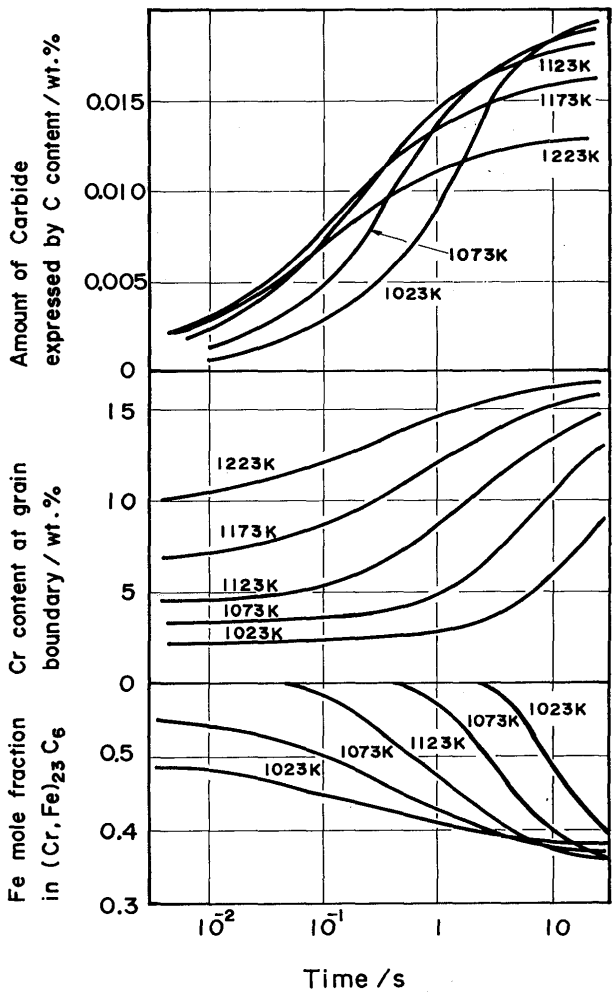

Fig. 2 Calculated results for SUS430.
(17.0Cr-0.02C, grain size: 8)

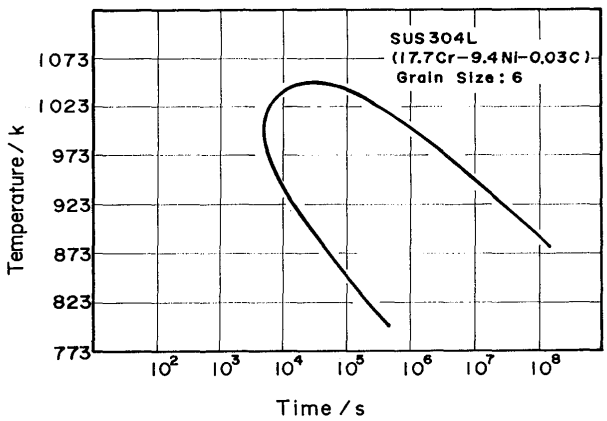

Fig. 3 Calculated TTS diagram for SUS304L.

the short-time side and had high nose temperature compared with the austenitic one. This is because of a low solubility of C and a high diffusion rate of Cr. These curves explain the fact that low C ferritic stainless steels are not easily prevented from intergranular corrosion by welding.

5. Lowering the Carbon Content of 17Cr Steel

There is a strange phenomenon that 17Cr stainless steel becomes more susceptible to intergranular corrosion when its carbon and nitrogen contents are decreased. It has been explained that with the increase in the C and N contents, the steel creates an austenitic phase which works as an absorbent for C and N and lowers the C and N contents in the ferrite, therefore the precipitation of carbide is inhibited[1]. However, this theory does not hold well from a view point of phase diagram. It is of no doubt that the phenomenon is closely related to the existence of austenite, but more stringent examination will be required.

5.1 Effects of C and N

The effects of C and N on welded 17Cr stainless steel were examined. The chemical compositions are shown in Table 1. Ingots of 5 kg weight were rolled to sheets of 1.0 mm thick by way of hot and cold rolling. Welding was performed by TIG (a current of 60–80 Amp. and a velocity of 0.5 m/min). The quantity of martensite was

measured in the bead zone. Corrosion tests were performed by way of Strauss test (JIS), a chloride environment corrosion test (3000 ppm Cl^-; 0.15% $Na_2Cr_2O_7 \cdot 2H_2O$, at 85°C for 4 months), and a weathering test (in Sagamihara city, for 6 months). Results are also given in Table 1. As obvious from the results, the 17Cr steel gets remarkable intergranular corrosion at a C + N content of 0.04% or less. Metallographically, the intergranular corrosion increases more when the quantity of martensite in the bead is at 5% or less. The steel is somewhat recovered from the corrosion when C + N drops to a level as low as 0.013%.

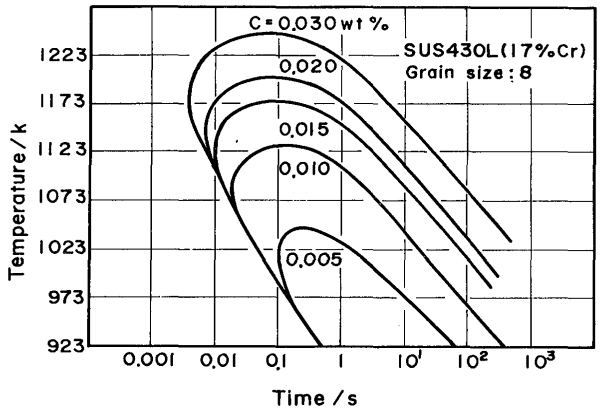

Fig. 4 Calculated TTS diagrams for various carbon content.

5.2 Calculated phase diagram

As concerns the phase diagrams for Fe-Cr-C steels, there are phase diagrams such as those reported by Bungardt et al.[5], Imai et al.[6),7)] and Uhrenius[8]. However, all of them are not practical as they lack the accuracy as to the data on the boundary between ferrite and ferrite + austenite or between ferrite and ferrite + carbide, i.e. the data on the extremely low-C side. Based on the thermodynamic data which have been described in Section 2 above, the calculated phase diagrams were attempted to make. As standard equation, set up equation (28) at the boundary between the ferrite + austenite and the austenite region, where data are relatively accurate, using data from some references[5)–10)]:

$$X_{Cr} = 4.41X_C + 0.122 - 7\times10^{-9}(T-1273)^2 \quad (28)$$

Figures 5–8 show the phase diagrams calculated for 1173K, 1273K, 1373K and 1473K.

5.3 Precipitation competition between carbide and austenite

As shown in Fig. 4, it is at 1173K that the intergranular corrosion in ferritic stainless steels causes the largest problem. Figure 5 shows a equilibrium phase

Table 1 Effect of carbon and nitrogen for intergranular corrosion sensibility in 17 Cr stainless steels.

No.	Composition (wt. %)						Martensite in weld (%)	Corrosion test		
	C	Si	Mn	Ni	Cr	N		Strauss*	Chloride**	Weather***
1	0.006	0.50	0.43	0.18	16.23	0.007	0	XX	○	△
2	0.032	0.52	0.44	0.19	16.39	0.007	1.7	XX	X	X
3	0.034	0.49	0.43	0.20	16.48	0.008	0.2	XX	X	X
4	0.050	0.52	0.47	0.20	16.46	0.007	6.3	△	○	○
5	0.078	0.53	0.77	0.10	16.81	0.007	22.1	△	○	○
6	0.006	0.46	0.40	0.20	16.23	0.015	0	XX	X	X
7	0.018	0.31	0.27	0.21	16.35	0.012	0.9	XX	X	X
8	0.060	0.57	0.41	0.36	16.31	0.019	16.6	△	○	○
9	0.062	0.48	0.51	0.24	16.28	0.015	19.4	△	○	○
10	0.068	0.47	0.38	0.20	16.08	0.016	29.1	△	○	○
11	0.020	0.43	0.39	0.20	15.70	0.019	0.5	XX	X	X
12	0.026	0.46	0.40	0.21	14.41	0.012	6.8	X	○	○
13	0.028	0.75	0.43	0.20	16.01	0.013	1.0	XX	X	X
14	0.024	1.23	0.36	0.19	16.33	0.015	0	XX	X	X

XX : severely attacked
X : attacked
△ : slightly attacked
○ : good

* Strauss test (JIS)
** 3000 ppm Cl^- + 0.15% $Na_2Cr_2O_7 \cdot 2H_2O$ at 85°C
*** Weathering test at Sagamihara

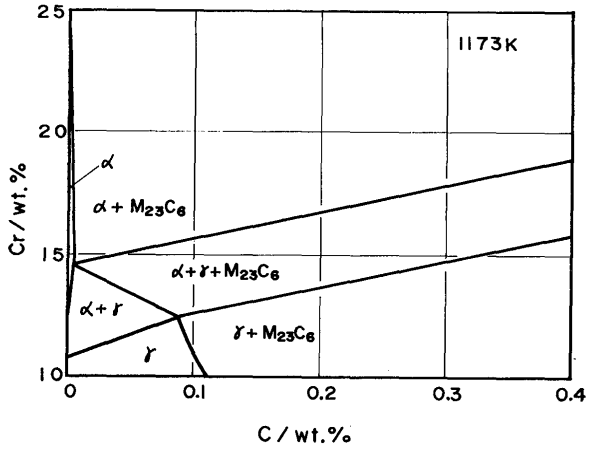

Fig. 5 Calculated Fe-Cr-C phase diagram at 1173K.

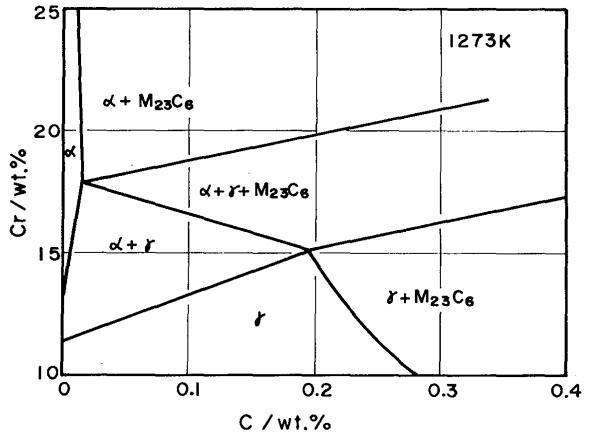

Fig. 6 Calculated Fe-Cr-C phase diagram at 1273K.

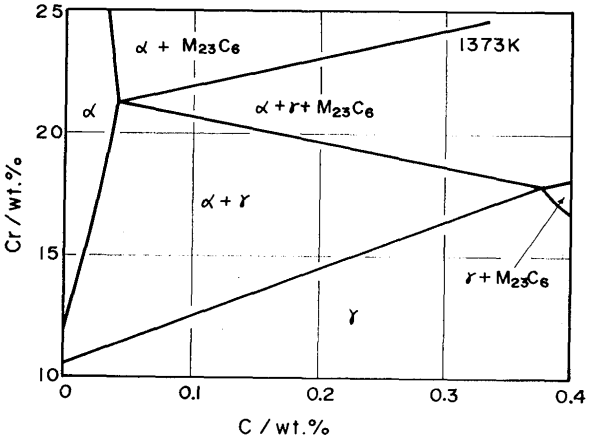

Fig. 7 Calculated Fe-Cr-C phase diagram at 1373K.

diagram for 1173K. In the case of 17%Cr, there is no austenite as a stable phase below about 0.2%C. However the austenitic phase is often observed at 1173K in practically used 17Cr stainless steel. Therefore the austenitic phase may be considered as a metastable phase. Namely, which precipitation of either carbide or austenite occures depends on thermal history.

In order to make it easy to understand this problem, let us superpose the phase diagrams for 1473K and 1173K in **Fig. 9**, cosidering a heat cycle by welding.

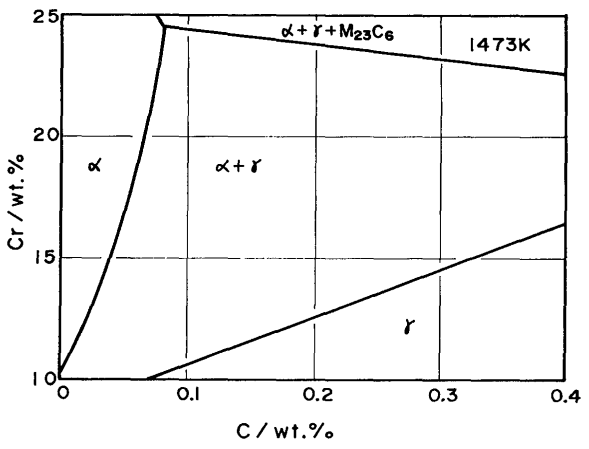

Fig. 8 Calculated Fe-Cr-C phase diagram at 1473K.

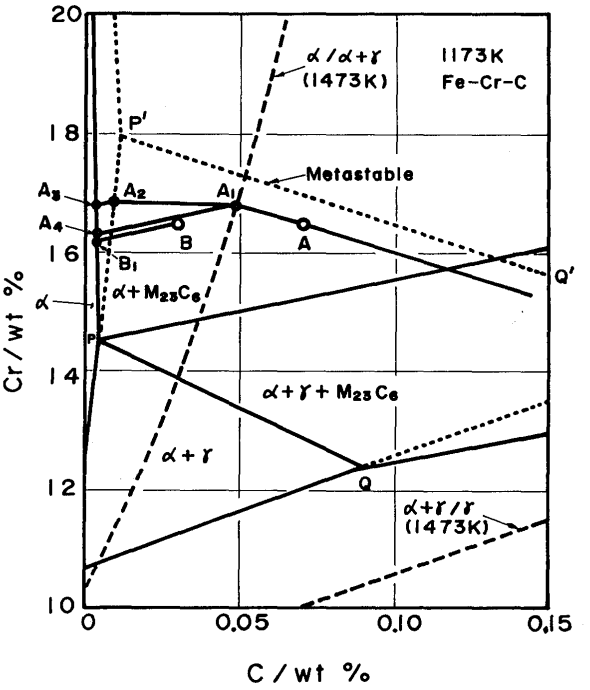

Fig. 9 Possible phase transformations from 1473K to 1173K in 17Cr-lowC stainless steel.

Now let us take up 16.5% Cr stainless steels with a C content of 0.07% (Steel A) and 0.03% (Steel B), respectively. In this case, Steel A at 1473K creates about 10% austenite and the ferritic phase composition equilibrates to the point A_1 of Fig. 9, where C content is down to 0.05%. On the other hand, in the case of Steel B, a single phase of ferrite is maintained at 1473K, and all of C is in solid solution. Let us assume that the temperature goes down to 1173K. Steel B just changes the solubility limit of C for that temperature (point B_1) with carbides ($M_{23}C_6$) precipitation. Meanwhile, the ferritic phase of Steel A, on facing the temperature drop, takes the following two ways which compete with each other: (1) The ferrite reaches the metastable point A_2, precipitating a new austenitic phase around the already existing austenitic phase, and then heads for point A_3, precipitating carbide; or (2) the ferritic phase directly heads for

point A_4 from A_1, precipitating carbide. In the latter case, carbide precipitation requires nucleus formation, but the precipitation of austenitic phase is advantageous in that new austenite can grow adjacent to the pre-existing austenite. Thus, the austenite precipitation needs only small formation energy, saving the nucleus-forming energy (surface tension energy).

Now r represents the radius of nucleus, represents the surface tension energy, and V_θ represents the molar volume (the volume per mole of metal component, same as equation (18)) of the precipitate, then the energy required for nucleus formation is given by

$$E = 2\sigma V_\theta / r$$

Now let us assume $\sigma = 0.7\,\mathrm{J/m^2}$, $V_\theta = 7 \times 10^{-6}\,\mathrm{m^3/mole}$, and r is 2 to 5 nm, then E is calculated in the range of 2000 to 5000 J/mole. With E being tentatively set at 2500 J/mole, the metastable phase diagram at 1173K was recalculated, as shown in Fig. 9, where the line PQ shifts to the line P'Q'. It means that the Steel A precipitates metastable austenite more than the carbide, because carbide precipitation needs nucleus formation energy. Thus, the steel precipitates austenite down to point A_2, and then it starts precipitating carbide. In that case, carbide precipitation starts at a carbon content of 0.008% in Steel A, far less than 0.03% for Steel B. Despite C content is 0.07%, Steel A has substantially the same effect as the C content is below 0.008%. Moreover, Steel A is advantageous in that, during the period in which it is precipitating the metastable austenite, incubation period can be extended as much as that precipitating period. Thus, clear explanation can be made for the phenomenon of intergranular corrosion acceleration caused by the decrease in the C and N contents of 17Cr stainless steel.

Figure 10 shows the growth of new austenite around the austenitic phase existing equilibriumly at 1473K during the cooling period. The sample used is 15Cr-0.07C stainless steel which has been heated to 1473K for 70 hr and then cooled in the air.

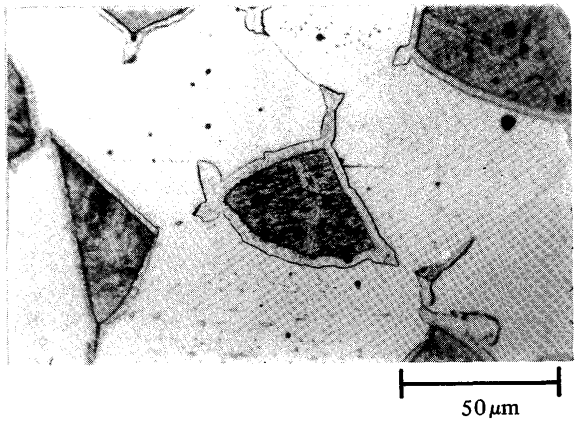

Fig. 10 Metastable precipitated austenite around the original austenite formed at 1473K in 15Cr-0.07C stainless steel.

6. Conclusions

Theoretical study on the carbide precipitation and the susceptibility to intergranular corrosion in ferritic stainless steel were performed, and obtained the following results:

(1) The activities of Cr, Fe and C in stainless steels were gathered and chekced, and carbide precipitation at grain boundary was calculated by using a local equilibrium model. It has been found that ferritic stainless steel is 10^5 times as susceptible to intergranular corrosion as austenitic stainless steel.

(2) It is demonstrated that the lower the C content of ferritic stainless steel, the more susceptible it becomes to intergranular corrosion. It is also showed that the cause of corrosion depends on whether austenitic phase is created or not in the steel at the time of welding.

(3) As to the reason why the creation of austenite makes the steel less susceptible to intergranular corrosion, it is explained by a competitive relationship between carbide precipitation and austenite transformation in a supersaturated state during the cooling period, namely it is easier for the steel to transform into a metastable austenitic phase than to precipitate carbide, when an austenitic phase has been already present in the steel.

REFERENCES

1) T. Okazaki, T. Miyoshi, H. Abo and T. Hirai: Tetsu to Hagane (Iron and Steel, Japan) **63** (1977), 631.

2) T. Arai and S. Takeda: ibid, **72** (1986), 831.

3) A. D. Kulkarni and W. L. Worrell: Metall. Trans., **3** (1972), 2363.

4) H. B. Aaron, D. Fainstein and G. R. Kotler: J. Appl. Phys., **41** (1970), 4404.

5) K. Bungardt, E. Kunze and E. Horn: Arch. Eisenhuttenwes., **29** (1958), 193.

6) Y. Imai, K. Masumoto and M. Naga: Nippon Kinzoku Gakkaishi (J. Japan Inst. Metals), **30** (1966), 747.

7) Y. Imai, K. Masumoto and M. Naga: ibid, **29** (1965), 860.

8) B. Uhrenius: Hardenability concepts with Applications to Steel, Metallurgical Society of AIME, (1978), 28.

9) E. Baerlecken, W. A. Fisher and K. Lorenz: Stahl und Eisen, **81** (1961), 768.

10) T. Suzuki: A study on two-phase austenitic/ferritic stainless steel (doctor's thesis, Osaka University), (1967).